

Intraband relaxation in CdSe nanocrystals and the strong influence of the surface ligands

Philippe Guyot-Sionnest,^{a)} Brian Wehrenberg, and Dong Yu
James Franck Institute, 5640 South Ellis Avenue, Chicago, Illinois 60637

(Received 28 April 2005; accepted 27 June 2005; published online 25 August 2005)

The intraband relaxation between the $1P_e$ and $1S_e$ state of CdSe colloidal quantum dots is studied by pump-probe time-resolved spectroscopy. Infrared pump-probe measurements with ~ 6 -ps pulses show identical relaxation whether the electron has been placed in the $1S_e$ state by above band-gap photoexcitation or by electrochemical charging. This indicates that the intraband relaxation of the electrons is not affected by the photogenerated holes which have been trapped. However, the surface ligands are found to strongly affect the rate of relaxation in colloid solutions. Faster relaxation (< 8 ps) is obtained with phosphonic acid and oleic acid ligands. Alkylamines lead to longer relaxation times of ~ 10 ps and the slowest relaxation is observed for dodecanethiol ligands with relaxation times ~ 30 ps. It is concluded that, in the absence of holes or when the holes are trapped, the intraband relaxation is dominated by the surface and faster relaxation correlates with larger interfacial polarity. Energy transfer to the ligand vibrations may be sufficiently effective to account for the intraband relaxation rate. © 2005 American Institute of Physics. [DOI: 10.1063/1.2004818]

I. INTRODUCTION

Electronic relaxation is one of the basic issues in the area of nanomaterials. With the high surface-to-volume ratio, the surface properties are expected to be important. This is well established for the case of conduction to valence-band recombination in semiconductor quantum dots, where nonradiative processes are mostly due to carrier traps at the surface. Indeed, with surface control and core-shell samples, materials with band gaps in the UV-visible and near-infrared regimes can exhibit high photoluminescence efficiency.

In contrast, the relaxation of carriers between the quantum states within a band, either the valence or conduction band, *intraband* relaxation, is systematically in the picosecond or subpicosecond regime,^{1,2} 10^6 times faster than the estimated radiative lifetimes.

This rapid intraband relaxation rate is relevant to several applications. It is actually necessary for interband lasing, as it allows rapid population of the lowest states from which light is emitted.³ On the other hand, the intraband transitions could be used for mid-infrared light sources and detectors if the relaxation rates were significantly slower.

Colloidal nanocrystals have well-defined intraband transitions.⁴ In these nearly spherical quantum dots, the transition between the $1S_e$ and $1P_e$ electronic states is tunable throughout the mid-infrared as a function of size. The transition has a large optical cross section,⁴ a narrow homogeneous width,⁵ and it can be turned on by photoexcitation or carrier injection.⁶ To date, the intraband transitions in these quantum dots remain of academic interest because the lifetime of the $1P_e$ state is in the picosecond range, many orders of magnitude shorter than a radiative recombination time or tunneling time.

This paper provides the first experimental data where a different surface preparation is shown to lengthen the $1P_e$ state lifetime by several orders of magnitude compared to previous results.¹

II. BACKGROUND

Intraband relaxation in quantum dots should be quite distinct from energy relaxation in the bulk. In bulk semiconductors, there is a continuum of electronic states and the energetic carriers lose their energy by emitting optical phonons, with energy relaxation rates of the order of 0.5 eV/ps.¹ However, in quantum dots, the discrete energy levels modify the relaxation rate and mechanism.

For quantum dots of weak confinement energies, < 0.1 eV in most materials, the electronic states are separated by only one or two optical-phonon energies. The electronic states are therefore strongly coupled via the optical phonons and may be better described as polarons.⁷ The relaxation rate is then dominated by the phonon lifetime themselves which is of the order of tens of picoseconds.

In strongly confined quantum dots, the electronic states are separated by several multiples of $\hbar\omega_{LO}$, 0.03 eV for CdSe, and coupling to the optical phonons cannot compensate for the large energy mismatch. This is the regime of the *phonon bottleneck*, where phonons should not account for the energy relaxation.^{3,8} This should lead to very long relaxation times. However, very fast intraband relaxation is the general observation.

To explain the fast relaxation, a mechanism has been proposed where the electrons relax via their strong Coulomb interaction with the holes.^{9,10} The strong overlap of the holes and electrons further enhances this effect in the quantum dots. For III-V and II-VI materials, the high mass of the hole and the threefold band degeneracy of the valence band still lead to weak confinement of the hole state, and hole energy

^{a)}Electronic mail: pgs@uchicago.edu

relaxation can therefore proceed via phonon-mediated processes. In agreement with this mechanism, colloidal CdSe quantum dots that are photoexcited in the P excitonic state exhibit an ultrafast relaxation to the S exciton in the subpicosecond regime. An energy relaxation rate of ~ 1 eV/ps has been observed, increasing for smaller dots.¹ Theoretical relaxation times with this mechanism range from ~ 100 ps (Ref. 9) to a few picoseconds¹⁰ and even tens of femtoseconds,¹¹ and encompass all measurements to date.

With this mechanism, the fast relaxation should be avoidable if the quantum dot has only electrons or if both holes and electrons have similarly sparse density of states.

These situations have been tested experimentally. For epitaxially surface-grown quantum dots, many reports have similarly shown very fast excitonic relaxation. In one instance, surface-grown quantum dots were engineered such that the electron-hole pairs would separate with the electrons confined into the quantum dots, while the hole remained in the wetting layer.¹² A very slow intraband relaxation, 750 ps, was reported although this result has not been confirmed by other groups.

For the colloidal systems, the results have been inconclusive. Experiments have been performed on colloidal quantum dots where the surface has been modified to provide a trapping site for the hole after photoexcitation of the electron-hole pair. Thus, thiophenol and pyridine, which act as hole traps, could slow down the $1P_e-1S_e$ relaxation to about 2–3 ps,^{13,14} which is qualitatively consistent with the electron-hole Auger mechanism. However, one should expect a much larger decrease of the coupling as the hole moves from a delocalized hole state to a surface-trapped state, and it is therefore surprising that the lifetimes were not longer than a few picoseconds.

It has also been observed that highly fluorescent IV-VI nanocrystals exhibit fast intraband relaxation.² Yet, the IV-VI PbSe nanocrystals have similar hole and electron masses and density of states and, thus, it is unlikely that the Auger relaxation mechanism could still explain the fast relaxation in these systems.

Finally, reduced colloidal nanocrystals have been investigated to specifically test the role of the hole. Using a strongly reducing agent such as sodium biphenyl, electrons were injected in the $1S_e$ state of the nanocrystals.⁶ Pump-probe experiments carried out on the $1S_e-1P_e$ infrared transition have led to similar intraband relaxation rate as when the electrons were photoexcited. N -type ZnO and CdSe colloidal nanocrystals showed resolution-limited relaxation lifetimes of < 5 ps even down to 6 K.⁵ N -type InP also showed fast relaxation of the order of 3–8 ps,¹⁵ similar to that of photoexcited nanocrystals. These results on n -type nanocrystals indicate most clearly that, in the absence of a free hole, another efficient mechanism must lead to the fast intraband relaxation.

III. EXPERIMENTAL RESULTS

A. Electrochemical reduction

Electrochemical reduction of nanocrystals deposited on an electrode is an improved means of electron injection

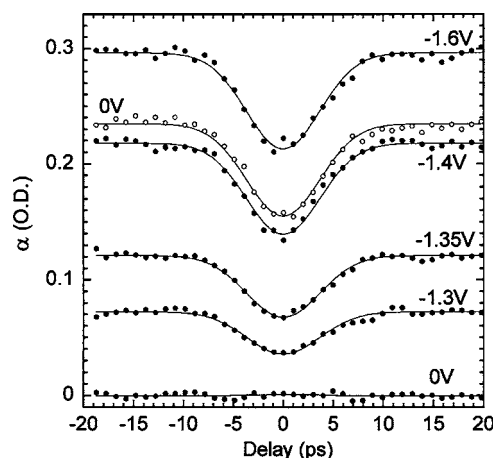


FIG. 1. Infrared absorbance as a function of IR pump-probe delay for a film of CdSe nanocrystal (~ 6 -nm diameter) at the indicated potentials, solid circles. The open circles, the same but with a 532-nm pump pulse 350 ps earlier. The potentials are referenced to a Ag wire pseudoreference. The electrolyte is CH_3CN and tetrabutyl ammonium perchlorate. The zero delay is arbitrary.

where the average electron occupation can be accurately dialed.¹⁶ Figure 1 shows the results from a pump-probe experiment for electrochemically reduced nanocrystals. The infrared probe signal is obtained in reflection from a film of CdSe nanocrystals bound to an indium tin oxide (ITO) electrode. The film has been treated with hexanedithiol to provide a fast and complete electrochemical response¹⁷ and the sample is cooled to -60 °C to improve the electrochemical stability. Both pump and probe pulses have the same wavelength of $5 \mu\text{m}$, approximately resonant with the peak of the inhomogeneously broadened $1S_e-1P_e$ intraband absorption for this size of nanocrystals (~ 6 nm). As the potential is made more negative, electrons occupy the $1S_e$ state and the infrared probe beam intensity diminishes due to the $1S_e-1P_e$ absorption as shown by the increased absorbance shown in Fig. 1. Around zero delay, the infrared pump beam induces a bleach which is essentially proportional to the absorbance. Because the intraband relaxation is faster than the pulse widths (~ 6 ps), the bleach response is effectively limited by the pulse widths. However, the relative amplitude of the bleach, at identical pump power, must be strongly affected by the lifetime. It is then noteworthy that, for all degrees of reduction, the relative bleach amplitude is the same.

This experiment demonstrates that fast intraband relaxation is observed even in the absence of holes, confirming the results previously obtained for chemically reduced nanocrystals. This fast intraband relaxation cannot be explained by the coupling of the electrons and holes and, thus, must be associated with another mechanism.

Reversible electrochemical charge injection further allows the direct comparison between the intraband relaxation in the charged state, in the absence of holes, or after photoexcitation of the neutral state, where cooled or trapped holes are present. In thiol-treated CdSe nanocrystals that have been photoexcited, the hole is rapidly trapped, presumably by the sulfur lone pair, while the electrons remain in the delocalized $1S_e$ state. Thus, 350 ps after exciting the neutral film with a 532-nm pulse, the electron has relaxed to the $1S_e$ state, while

the hole is in a surface trap. As shown in Fig. 1, the infrared pump-probe response is indistinguishable from the case of the charged films. This similarity of the bleach in width and magnitude implies that trapped holes, which are created by the 532-nm pulse, have no noticeable effect on the intraband relaxation.

In prior experiments, treating the surface with hole-trapping thiophenol or pyridine ligands was observed to lead to slightly slower intraband relaxation from ~ 0.3 ps (Ref. 1) to less than 3 ps.^{13,14} The increase was understood in the context of the electron-hole Auger coupling mechanism, where the trapped hole led to a reduced coupling and slower relaxation rate. It is now apparent that the trapped hole may not have participated in the relaxation rate and another mechanism led to the remaining picosecond relaxation time.

B. Surface modification

Having ruled out that the trapped hole or the optical phonons are responsible for the picosecond intraband relaxation, surface electronic or vibrational excitations remain likely candidates. The surface of colloidal quantum dots is a mostly uncharacterized system, with multiple bonding geometries of surface atoms, typically a cocktail of surface ligands, and physisorbed impurities attracted to the polar core. While it is well established that the surface plays an essential role in the interband relaxation,¹⁸ where carrier trapping on picosecond time scales can efficiently compete with radiative lifetimes of nanoseconds, little attention has been given to surface effects for the intraband relaxation.¹⁹

In the following experiments, CdSe nanocrystals of varied sizes and surface chemistries have been investigated. For the cap exchange, a small amount of the reaction mixture is dissolved in chloroform and precipitated once in methanol. The solid precipitate (~ 20 mg) is dissolved in 1-ml hexane and mixed with 2 g of the ligands. Tetradecylphosphonic acid (TDPA), oleic acid (OAcid), oleylamine (OLA), and *n*-dodecanethiol (DDT) have been investigated. To facilitate cap exchange for DDT, OLA, and OAcid, the solution of ligands and nanocrystals is heated to 80 °C for 5 min under vacuum. Under argon, the temperature is then rapidly ramped up to 220 °C before the heating mantle is removed. The large excess of the new ligands and the high temperature should facilitate the exchange. The short time, on the order of a minute, at the high temperature is necessary to limit the broadening of the size distribution of the nanocrystals. After cooling back to room temperature, the sample is precipitated with methanol, dried under vacuum, and dissolved in tetrachloroethylene (C_2Cl_4). The sample is loaded into a cell with sapphire windows with a gap of 0.4 mm. The optical density at the 1S exciton is adjusted to be between 1 and 1.5.

To populate the $1S_e$ state, an 8-ps pump pulse at 532 nm first excites the solution of colloidal nanocrystals. The probe pulses are derived from a parametric optical amplifier (~ 6 -ps pulses tunable from 450 to 700 nm).

As shown in Fig. 2, the 532-nm pump induces a strong bleach of the optical density (OD) of typically $\Delta OD_{1S} \sim 0.5$ at the first exciton due to the long-lived (>1 ns) electron in the $1S_e$ state.

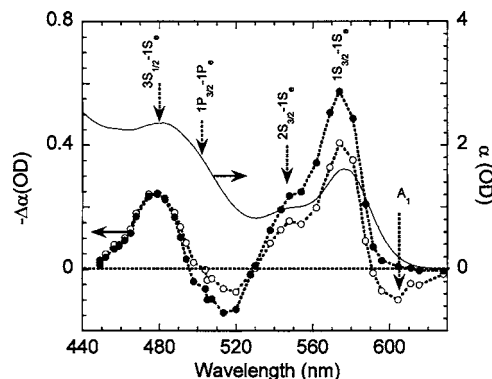


FIG. 2. Optical absorption for a CdSe sample with the 1S exciton peak at 575 nm (~ 4.5 -nm diameter), solid line. The solid circles are the changes in optical density when a 532-nm pump pulse excited the sample 350 ps before the visible probe. For this sample, $1S_{3/2}-1S_e$ is at ~ 575 nm, $2S_{3/2}-1S_e$ at ~ 550 nm, and $3S_{1/2}/1S_e$ at ~ 480 nm. $1P_{3/2}/1P_e$ is at ~ 510 nm. The open circles represent the changes in optical density when the sample was also excited by an infrared pump pulse at $4 \mu\text{m}$, 10 ps before the probe.

The occupation of the $1S_e$ state bleaches transitions to other states as well as giving features assigned to $1S_{3/2}-1S_e$, $2S_{3/2}-1S_e$, and $3S_{1/2}/1S_e$.²⁰ There is also a strong induced absorption, which is dominantly assigned to a redshift of the $1P_{3/2}/1P_e$ absorption. The assignment of the spectral features are taken from similar studies by Klimov *et al.*²¹

While the visible 532-nm pump is maintained 350 ps before the visible probe, the sample is then excited by an infrared pump pulse ($\sim 10 \mu\text{J}$, ~ 6 ps). The infrared pump is resonant with the intraband transition, $1S_e-1P_e$, and this allows to single out the electron dynamics.¹⁵ For samples with slow intraband relaxation, the infrared pump pulse can generate changes as large as 60% of the $1S_e$ state population as seen in the change of $\Delta OD_{1S_{3/2}-1S_e}$, but typically the changes are in the 10%–30% range as in Fig. 2. Most of the features are associated with reduction of the $1S_e$ state population. However, on the red edge of the 1S exciton, noted A_1 , the induced absorption is specifically associated to a redshift of the 1S exciton due to the occupation of the $1P_e$ state.²¹ The infrared-induced bleach in the P -exciton range is also partly associated with the occupation of the $1P_e$ state.

Rather than returning to the $1S_e$ state, the electron may also fall into a trap state or recombine with trapped holes. These other pathways will appear as long-lived infrared-induced effects. They are the likely explanations for the long-lived IR pump-probe bleach response reported in earlier experiments.^{13,5} Tuning the visible probe either to the P -exciton region, the infrared-induced bleach around 510 nm for the size of nanocrystals in Fig. 2, or below the S -exciton, the infrared-induced absorption A_1 feature at 605 nm, allows to minimize the effect and extract more cleanly the intraband relaxation rate. Both methods yield identical relaxation times.

Figure 3 shows the relaxation of nanocrystals prepared following the original TOP/TOPO procedure²² and then treated to modify the ligand shell. The ~ 5 -nm diameter nanocrystals have the $1S_{3/2}-1S_e$ exciton around 595 nm and the $1S_e-1P_e$ transition around $4.5 \mu\text{m}$. In the order of increasing relaxation time, the surface ligands tested are TOP/TOPO, oleic acid, oleylamine, and *n*-dodecanethiol. Samples

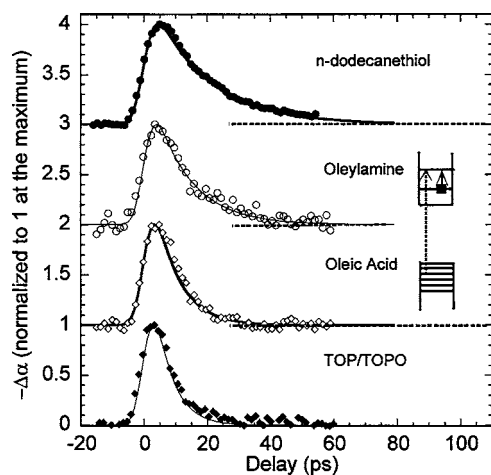


FIG. 3. Normalized pump-probe response of ~ 5 -nm TOP/TOPO CdSe nanocrystals processed in different ligands and dissolved in C_2Cl_4 . The lines are visual best fits with a single exponential response to a Gaussian pulse at zero delay. From the bottom to the top, original TOP/TOPO nanocrystals (6 ps), oleic acid (8 ps), oleylamine (12 ps), and *n*-dodecanethiol (18 ps). As shown in the schematic, the infrared pump ($4.56 \mu m$) is in the $1S_e-1P_e$ intraband transition band and the probe is at 540 nm in the P -exciton band. The induced absorption are offset and normalized to 1. The magnitudes, which are not shown, follow the same trend as the relaxation times, increasing from bottom to top.

treated with *n*-dodecanethiol exhibit systematically the slowest relaxation. It was found that treating the TOP/TOPO nanocrystals in pure *n*-dodecanethiol at $70^\circ C$ led to relaxation times of ~ 10 – 13 ps, while the more rigorous heating under argon up to $220^\circ C$ increased it to 17 ± 3 ps.

Over the past few years the synthesis of CdSe nanocrystals has evolved significantly. In particular, the use of ionic Cd sources²³ and the exploration of other ligands, notably alkylamines,²⁴ have led to materials with similar size control but vastly improved luminescence. Highly fluorescent and monodispersed nanocrystals were therefore synthesized following literature procedure, starting with cadmium acetate, TOPSe, and a mixture of stearic acid, octadecylamine, and technical grade TOPO.²⁴ These samples exhibit a more systematic and extensive effect of surface modification on the relaxation rate as compared to the samples prepared by the previous method.

Figure 4 shows the relaxation measured for the unmodified sample presumably capped by octadecylamine and samples treated under mild heat ($70^\circ C$) in air in tetradecylphosphonic acid or under Ar at $220^\circ C$ in *n*-dodecanethiol. The trend is similar to that in Fig. 3. The phosphonic acid decreases the lifetime, while the dodecanethiol leads to an increase and the longest lifetime is now ~ 27 ps for the thiol-treated sample.

No correlations have been observed between the sample fluorescence and the relaxation time. In the data of Fig. 4, the original amine-capped sample is strongly fluorescent while both the TDPA and DDT samples are much less fluorescent, the DDT sample being the least fluorescent.

1. Size dependence

There seems to be a strong but nonmonotonous size dependence. With identical *n*-dodecanethiol surface-recapping

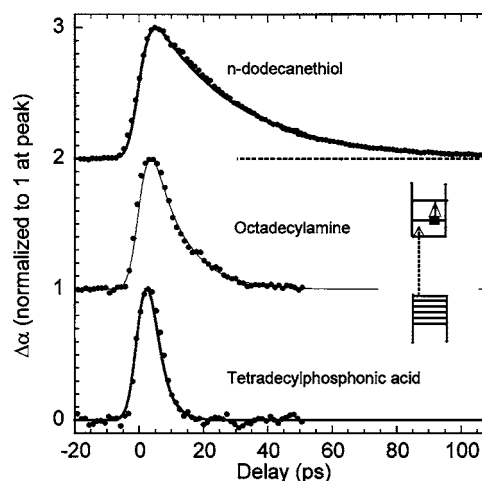


FIG. 4. Normalized pump-probe response of ~ 4.5 -nm octadecylamine CdSe nanocrystals (575-nm exciton peak) processed in different ligands and dissolved in C_2Cl_4 . The lines are visual best fits with a single exponential response to a Gaussian pulse of 6-ps full width at half maximum (FWHM), from bottom to top, 3.8, 10, and 27 ps. The infrared pump ($3.81 \mu m$) is in the $1S_e-1P_e$ band and the probe is at 605 nm in the A_1 feature. The absorption at 605 nm is increased by the infrared pump. The induced absorptions are offset and normalized to 1. The magnitudes which are not shown follow the same trend as the relaxation times, increasing from bottom to top.

procedures, larger samples of ~ 6 -nm diameter (exciton peak at 626 nm and pumped at 1800 cm^{-1}) showed predominantly a fast (~ 6 ps) relaxation. A relaxation rate of 29 ± 2 ps has been measured on samples of 5.4-nm diameter (exciton peak at 606 nm) pumped at $\sim 2000 \text{ cm}^{-1}$. At smaller sizes, no infrared pump-induced effect could be observed for a sample of 3.3 nm (exciton peak at 527 nm) pumped at $\sim 3200 \text{ cm}^{-1}$, possibly indicating a very short lifetime.

2. Temperature dependence

Reducing the temperature should help slow down energy relaxation rates in cases where low-frequency vibrations are involved, such as in charge transfer. In one previous experiment only a small increase in lifetime was reported.¹³ Measuring the relaxation rate at low temperature is rendered difficult by the need of a clear matrix. C_2Cl_4 is very foggy at 15 K. However, using a thin cell of 50- μm thickness, a sufficient probe signal could be transmitted. Although the data were very noisy, the relaxation rates at 15 K appeared similar to room-temperature data. Dodecanethiol-recapped CdSe nanocrystals are not very soluble in the glass-former heptamethylnonane, tending to aggregate as the sample is cooled down or laser irradiated. Nevertheless, a sample remained sufficiently clear at 15 K to perform the measurement. The data are shown in Fig. 5. The initial relaxation is faster at low temperature, but the slow tail remains. Samples treated with octadecylamine, which are well soluble in HMN, did not exhibit significant difference in the relaxation rate at low temperatures.

IV. DISCUSSION

The novel result of this work is that surface modification strongly affects the intraband relaxation, leading to much longer intraband relaxation times than previously reported.

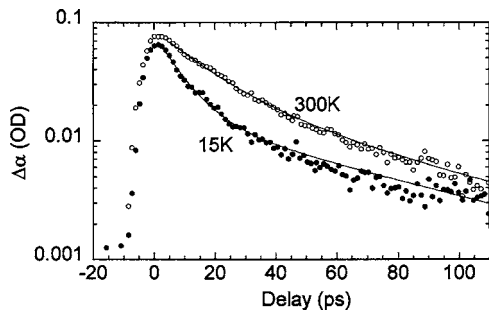


FIG. 5. Pump-probe response of CdSe with a 606-nm exciton treated with *n*-dodecanethiol and dissolved in the low-temperature glass-former heptamethylnonane. 300 K, open circles, biexponential fit with 17 and 65 ps. 15 K, solid circles, biexponential fit 8.5 and 65 ps. The sample is brightly fluorescent at 15 K.

The energy relaxation which is mediated by the surface may involve electronic or vibrational processes and these are discussed separately.

A. Electronic mechanism

The ligands coordinate essentially to the surface Cd²⁺ ions. Their interaction with Cd²⁺ can be discussed in the context of the hard-soft acid-base theory used in inorganic chemistry. Cd²⁺ is a soft acid consistent with its large and polarizable ionic core. Base conjugates of phosphonic acid, R-PO₃H²⁻ and carboxylic acid R-CO₂⁻, where the lone pairs of the O atoms provide for the ligand interaction, are “hard” multidentate bases. Alkyl amines R-NH₂ are classified as bases intermediate between hard and soft due to the more polarizable N lone pair. RS⁻ are considered to be soft bases as the sulfur has the most polarizable lone pair. Experimentally, the intraband lifetime follows the trend RS⁻ > RNH₂ > R-CO₂⁻ ~ R-PO₃H²⁻, which is also in the order of increasing hardness. Therefore, slow relaxation correlates with softer ligands and decreased polarity of the metal ligand bond.

A likely candidate for electronic relaxation is charge transfer from the 1P_e state to a surface state such as the empty *s* orbital of the exposed surface Cd²⁺ atoms. For all ligands, the surface Cd²⁺ orbitals should be mostly above the 1S_e level, otherwise rapid electron trapping would occur. However, if this orbital is between the 1P_e and 1S_e states, it can shuttle the electrons between the 1P_e state and the 1S_e state. This “defect-assisted” mechanism for intraband relaxation was discussed by Schroeter *et al.* in the context of the surface-grown quantum dots.²⁵

The mechanism shown schematically in Fig. 6 is consistent with the observed trend that the softer ligands lead to a slower relaxation. Softer ligands form a more covalent bond with the Cd²⁺ orbital. This leads to a filled bonding orbital, of mostly ligand character, below the conduction band and an empty antibonding orbital, mostly Cd²⁺, that may be pushed higher than the 1P_e state. One difficulty with this mechanism is that there could be a strong temperature dependence associated to the role of low-frequency vibrations in the charge transfer, which so far has not been identified.

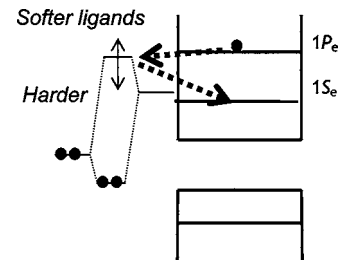


FIG. 6. Schematic of the potential role of surface Cd atoms in assisting the intraband relaxation and the role of surface ligands. As the softer ligands form a more covalent bond, the antibonding ligand-surface Cd orbital is moved higher in energy, beyond the 1P_e state.

B. Vibrational mechanism

The relaxation rate may also correlate with the infrared activity of the ligand shell, where the high-frequency vibrations associated with the ligands can serve as sinks to the intraband excitation. This is a peculiarity of the colloidal quantum dots compared to the surface-grown quantum dots, which are embedded in an all-inorganic matrix.

All the ligands share similar CH vibrational modes, and therefore, these high-frequency stretching vibrations (~3000 cm⁻¹) and bending vibrations (~1400 cm⁻¹) could not be responsible for the differing relaxation rates in the data shown in Figs. 3 and 4. Furthermore, these vibrational bands are narrow and do not overlap with the 2000–2400-cm⁻¹ intraband transitions in these samples.

As shown in Fig. 7(a) octadecylamine (ODA) and DDT show mostly CH absorptions. The NH stretch vibrations, at 3200–3400 cm⁻¹, are weak and narrow in the ODA spectra, while the SH stretch vibration, expected around 2700 cm⁻¹, is not detected in the DDT spectrum. On the other hand, OAcid and TDPA exhibit intense and broad absorption throughout the 1500–3500-cm⁻¹ range. The strongest absorber is TDPA, with the continuum likely arising from intramolecular hydrogen bonding.²⁶

The coupling of the 1S_e-1P_e electronic transition to the surface molecular vibrations can be direct via the wavefunction overlap. The lifetimes resulting from such a mechanism would rely on atomistic details and they are difficult to estimate.

Another mechanism for energy transfer to vibrations is by near-field infrared absorption. A simple estimate can be done using the field from the dipole of the 1S_e-1P_e transition centered in a spherical absorbing shell of radius *R* and of thickness Δ*R* ≪ *R* ≪ λ, where λ is the infrared wavelength in vacuum. Assuming an imaginary dielectric constant of the shell, ε'', the nonradiative lifetime is calculated to be (CGS units)

$$\frac{1}{T_{nr}} = \epsilon'' \frac{\Delta R p^2}{R^4 \hbar}, \quad (1)$$

where *p* is the screened transition dipole.

In the 2000–2500-cm⁻¹ range corresponding to the data in Figs. 2 and 3, it is the thin (~0.1 nm) polar Cd²⁺-ligand shell which could absorb. An estimate of ε'' for an absorbing polar material is based on water at 2200 cm⁻¹. It is ε''

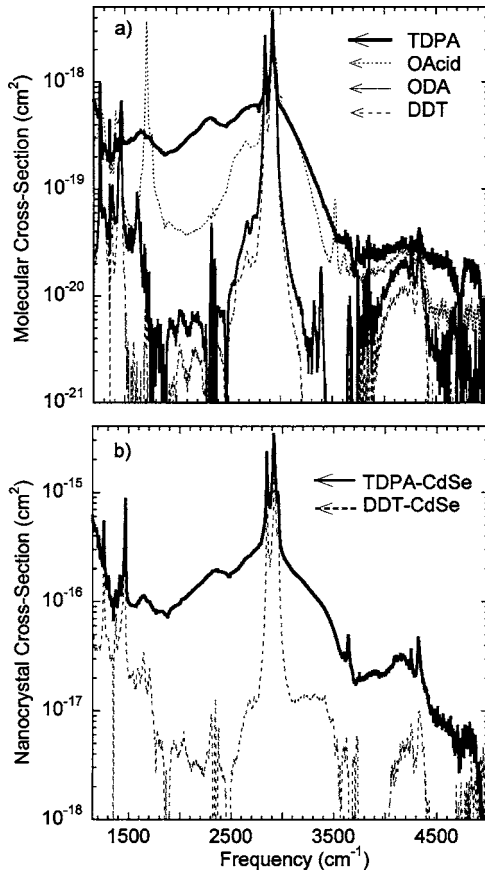


FIG. 7. (a) Infrared-absorption molecular cross sections of tetradecylphosphonic acid (TDPA), oleic acid (OAcid), octadecylamine (ODA), and dodecanethiol (DDT). The spectra are taken in C_2Cl_4 at $\sim 10^{-2}M$ concentrations. (b) Nanocrystal absorption cross sections for TDPA-treated CdSe and DDT-treated CdSe dissolved in C_2Cl_4 . The cross sections are obtained by normalizing to the $1S$ exciton cross section at 595 nm, taken to be $2.5 \times 10^{-15} \text{ cm}^2$. The log scale shows most clearly the difference in infrared activity of the varying surface ligands.

$=n\kappa\lambda/2\pi$, where κ is the inverse absorption length and n is the real index of refraction ($n=1.33$). At 2200 cm^{-1} for water, $\kappa=400 \text{ cm}^{-1}$ (Ref. 27) and $\varepsilon'' \sim 0.04$.

The screened transition dipole is $p=p_1(3\varepsilon_0)/(\varepsilon_1+2\varepsilon_0)$, where ε_1 is the sphere's optical dielectric constant ($\varepsilon_1 \sim 6$ for CdSe) and ε_0 is the surrounding dielectric constant ($\varepsilon_0 \sim 2.25$ for C_2Cl_4). The $1S_e-1P_e$ transition dipole is $p_1 \sim 0.3eR$.⁴

With these numbers and $R=2.25 \text{ nm}$, $T_{nr} \sim 16 \text{ ps}$ which is surprisingly fast. This estimate indicates that the lifetimes of mid-IR dipole-allowed transitions are seriously shortened by the presence of infrared-active materials in the nanocrystal shell.

A shell which absorbs the near-field infrared of the dipole should also be detectable in a far-field infrared-absorption spectrum of the solution. Indeed, the absorption of an infrared beam by the shell is calculated to have the cross section

$$\sigma_{\text{shell}} = 24\pi^2\varepsilon'' \frac{R^2\Delta R}{\lambda} \frac{(2\varepsilon_0^2 + \varepsilon_1^2)}{\varepsilon_0^{1/2}(\varepsilon_1 + 2\varepsilon_0)^2}. \quad (2)$$

With the parameters above leading to a lifetime of 16 ps, $\sigma_{\text{shell}} = 3 \times 10^{-18} \text{ cm}^2$. IR-absorption measurements of the

samples have been taken in C_2Cl_4 . Figure 7(b) shows the IR spectra of solutions of CdSe nanocrystals treated with TDPA and DDT. By several precipitations from methanol and vacuum drying, the solutions have been cleaned as well as possible to remove excess ligands. Nevertheless, the TDPA sample still shows the intense and broad IR absorption in the $2000-2500\text{-cm}^{-1}$ range, with cross sections in excess of 10^{-16} cm^2 . The DDT-capped CdSe samples show a much weaker IR absorption corresponding to cross sections in excess of 10^{-18} cm^2 . If these absorptions were associated with the Cd^{2+} -ligand interface, they would semiquantitatively account for the measured lifetimes.

This mechanism can explain why no infrared-induced pump effect was observed in the 3200-cm^{-1} range with CdSe nanocrystals of 3.3-nm diameter, and why shorter lifetimes were also observed for nanocrystals of 6-nm diameter probed around 1800 cm^{-1} , where the intraband transitions start to overlap with C-H stretching and bending modes and combination modes.

Furthermore, since the absorption of high-frequency molecular vibrations is not strongly affected by temperature, this mechanism suggests a weak temperature dependence as observed.

It is noteworthy that this near-field vibrational energy transfer, although slow compared to excitonic relaxation,¹ is still very fast compared to radiative lifetimes. It will in fact affect all transitions and not only dipole transitions, and it applies as well to interband²⁸ transitions.

For dipole transitions, the ratio of the radiative lifetime, T_1 , and nonradiative lifetime is

$$\frac{T_{nr}}{T_1} = \frac{32\pi^3\varepsilon_0^{1/2}}{3\varepsilon''} \left(\frac{R}{\lambda}\right)^3 \frac{R}{\Delta R}. \quad (3)$$

With the same parameters as above, $\varepsilon''=0.04$, $\lambda^{-1}=2200 \text{ cm}^{-1}$, $R=2.25 \text{ nm}$, $\Delta R=0.1 \text{ nm}$, and $\varepsilon_0=2.25$, $T_{nr}/T_1 \sim 0.3 \times 10^{-4}$, which implies a very small quantum yield. High-fluorescence quantum yields in the infrared range will therefore require great care in avoiding infrared absorption in the shell and matrix.

V. CONCLUSION

In summary, this work showed that the intraband relaxation rate of CdSe nanocrystals is much more strongly affected by the ligands than previously realized. The experimental results point to the direction of a more covalent interface accessible with "softer" ligands to lengthen the intraband relaxation time. For the $1P_e$ to $1S_e$ intraband transition around $4.5 \mu\text{m}$, the longest relaxation time obtained in this work is $\sim 30 \text{ ps}$. This is a couple orders of magnitude slower than the $\sim 0.3\text{-ps}$ relaxation time from the P to S excitons.¹

Concerning the mechanism for relaxation, the influence of the trapped hole has been observed to be negligible. This is in contrast to the case of excitonic relaxation,¹ where hot holes may still be the explanation for the subpicosecond relaxation. The alternative intraband relaxation mechanisms that have been proposed in this work involve energy transfer to electronic states mediated by the interfacial polarity or

energy transfer to high-frequency vibrations of the ligands. In particular, estimates of the energy-transfer rate to surface molecular vibration are rather consistent with the observations. It is expected that this mechanism should play a very significant role, and future work should investigate samples imbedded in a shell and a matrix free of high-frequency vibrations.

The slowest intraband relaxation time reported here is still approximately four orders of magnitude faster than radiative lifetimes. Slower relaxation should be possible with improved surface control. This might then open applications for the semiconductor nanocrystals in the mid-infrared.

ACKNOWLEDGMENTS

We would like to thank the US National Science Foundation (NSF) under Grant No. DMR-0407624 for funding. The authors made use of shared facilities supported by the NSF MRSEC Program under DMR-0213745.

- ¹V. I. Klimov, D. W. McBranch, C. A. Leatherdale, and M. G. Bawendi, *Phys. Rev. B* **60**, 13740 (1999).
- ²B. L. Wehrenberg, C. J. Wang, and P. Guyot-Sionnest, *J. Phys. Chem. B* **106**, 10634 (2002).
- ³H. Benisty, C. M. Sotomayor-Torres, and C. Weisbuch, *Phys. Rev. B* **44**, 10945 (1991).
- ⁴P. Guyot-Sionnest and M. A. Hines, *Appl. Phys. Lett.* **72**, 686 (1998).
- ⁵M. Shim and P. Guyot-Sionnest, *Phys. Rev. B* **64**, 245342 (2001).
- ⁶M. Shim and P. Guyot-Sionnest, *Nature (London)* **407**, 981 (2001).
- ⁷O. Verzelen, G. Bastard, and R. Ferreira, *Phys. Rev. B* **66**, 081308

- (2002).
- ⁸T. Inoshita and H. Sasaki, *Phys. Rev. B* **46**, 7260 (1992).
- ⁹I. Vurgaftman and J. Singh, *Appl. Phys. Lett.* **64**, 232 (1994).
- ¹⁰A. L. Efros, V. A. Kharchenko, and M. Rosen, *Solid State Commun.* **93**, 281 (1995).
- ¹¹M. Califano, A. Zunger, and A. Franceschetti, *Nano Lett.* **4**, 525 (2004).
- ¹²J. Urayama, T. B. Norris, J. Singh, and P. Bhattacharya, *Phys. Rev. Lett.* **86**, 4930 (2001).
- ¹³P. Guyot-Sionnest, M. Shim, C. Matranga, and M. A. Hines, *Phys. Rev. B* **60**, R2181 (1999).
- ¹⁴V. I. Klimov, A. A. Mikhailovsky, D. W. McBranch, C. A. Leatherdale, and M. G. Bawendi, *Phys. Rev. B* **61**, R13349 (2000).
- ¹⁵J. L. Blackburn, R. J. Ellingson, O. I. Micic, and A. J. Nozik, *J. Phys. Chem. B* **107**, 102 (2003).
- ¹⁶C. J. Wang, M. Shim, and P. Guyot-Sionnest, *Appl. Phys. Lett.* **80**, 4 (2002).
- ¹⁷P. Guyot-Sionnest and C. Wang, *J. Phys. Chem. B* **107**, 7355 (2003).
- ¹⁸G. Kalyuzhny and R. W. Murray, *J. Phys. Chem. B* **109**, 7012 (2005).
- ¹⁹Q. Darugar, C. Landes, S. Link, A. Schill, and M. A. El-Sayed, *Chem. Phys. Lett.* **373**, 284 (2003).
- ²⁰D. J. Norris and M. G. Bawendi, *Phys. Rev. B* **53**, 16338 (1996).
- ²¹V. I. Klimov, D. W. McBranch, C. A. Leatherdale, and M. G. Bawendi, *Phys. Rev. B* **60**, 13740 (1999).
- ²²C. B. Murray, D. J. Norris, and M. G. Bawendi, *J. Am. Chem. Soc.* **115**, 8706 (1993).
- ²³Z. A. Peng and X. Peng, *J. Am. Chem. Soc.* **123**, 183 (2001).
- ²⁴D. V. Talapin, A. L. Rogach, A. Kornowski, M. Haase, and H. Weller, *Nano Lett.* **1**, 207 (2001).
- ²⁵D. F. Schroeter, D. J. Griffiths, and P. C. Sercel, *Phys. Rev. B* **54**, 1486 (1996).
- ²⁶G. Zundel, *Adv. Chem. Phys.* **111**, 1 (2000).
- ²⁷G. M. Hale and M. R. Querry, *Appl. Opt.* **12**, 555 (1973).
- ²⁸J. M. Pietryga, R. D. Schaller, D. Werder, M. H. Stewart, V. I. Klimov, and J. A. Hollingsworth, *J. Am. Chem. Soc.* **126**, 11752 (2004).